

Energy Dissipation Characteristics of a Granular Flow Damper

S. C. Dragomir^{1,2}, M. Sinnott², S. E. Semercigil¹ and Ö. F. Turan¹

¹ School of Engineering and Science,
 Victoria University, Melbourne, Victoria 3000, Australia

²CSIRO Mathematics, Informatics and Statistics,
 Clayton, Victoria 3168, Australia

Abstract

The effectiveness of granular dissipation has been demonstrated earlier through experimental observations and simulations that use specified cylinder motion. Here, the development of a dynamic model is presented, where there is 2-way communication between the granular material and the container as a valuable design tool.

The objective of this progress report is to summarize the predictions obtained for a rotating granular dissipater, using the Discrete Element Method (DEM) technique. Comparisons are made with earlier work in which rotation of the boundary is specified.

Introduction

Tall structures require protection from transient forces such as those due to wind and earthquakes, for both structural safety and the comfort of the inhabitants. A variety of tuned mass dampers (TMD) are used to attenuate the excessive oscillations of such buildings. TMDs consist of a mechanism to transfer energy away from the structure (ensured by a tuning process) and dissipative elements. One such design of the authors uses a cylindrical container partially filled with a granular material which interacts with the structure through a circular track, as shown in Figure 1.

The efficiency of this design has been shown experimentally and numerically by Dragomir et al. [7-9]. The motion of the structure causes the cylinder to roll on the ramp, while the granular material inside the container experiences collisions with the boundary of the container and among its particles, resulting in energy dissipation.

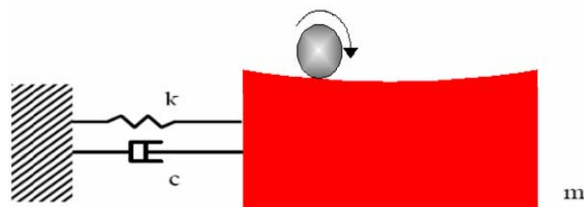


Figure 1. Proposed design with the cylindrical absorber for a structure of mass m , stiffness k and coefficient of damping c . When the structure experience a horizontal displacement, it causes the cylinder to roll on the ramp, while the granular flow of the particles inside dissipates the energy.

Particle-based numerical models are well suited to granular-flow devices since they are able to track the motion of each individual

particle and its interactions. The Discrete Element Method (DEM) is a particle-based method which has been reviewed by Campbell [2], Barker [1] and Walton [11]. A DEM granular solver developed by CSIRO is used here which has been successfully applied earlier to a wide range of applications from mining to pharmaceuticals (see Cleary [3,4] and Sinnott et al. [10] for examples).

The use of a dynamic model enables the simulation of granular sloshing absorbers without the need for experiments to define the motion of the device. A dynamic model allows the particle flow to modify the cylinder's motion and more physically predict the particle flow field, forces, and mechanisms of effective energy dissipation. Such predictions are essential to enhance the effectiveness of structure control and for implementing such devices on practical problem structures.

This work deals with a fully dynamic model of the cylinder rolling down a ramp with a no-slip condition at the ramp-cylinder interface. The basis of comparison is the specified motion case which yielded a good match of particle kinematics between the experiment and simulations [9].

Discrete Element Method

The DEM solver uses a linear spring-dashpot contact model and described in more detail by Cleary et al. [4]. Figure 2 is a simple schematic of the mechanical model. In the normal direction to the contact, the force F_n is

$$F_n = -k_n \Delta x + C_n v_n \quad (1)$$

where k_n and C_n are the contact stiffness and damping coefficients respectively, Δx is the amount of overlap, and v_n is the normal speed. The first term (the spring) in (1) represents the resistance to deformation, whereas the second term (the dashpot) is the equivalent viscous damping force, proportional to the normal speed. The spring is a purely repulsive force, to avoid non-physical attractive forces. The amount of particle overlap is determined by k_n .

The desired average overlap for the system should be less than 0.5% of the particle size. The damping coefficient C_n is dictated by the coefficient of restitution. In the tangential direction, the contact force is expressed as

$$F_t = \min(\mu F_n, k_t \int v_t dt + c_t v_t) \quad (2)$$

where μ is the friction coefficient, k_t and C_t are stiffness and damping coefficients respectively, and v_t is the speed in the tangential (shear) direction. The integral term represents the elastic deformation in the tangential direction. The total force is limited by the Coulomb force (μF_n). When it is reached, sliding of the contact surfaces begins.

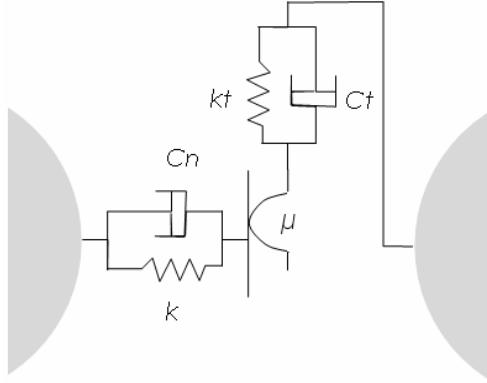


Figure 2. Schematic representation of DEM model.

Super-quadric shapes are used to model the particles as opposed to more commonly used spheres, as spheres cannot predict the shear resistance and dilation of particle beds accurately Cleary et. al [5,6]. The most general form of super-quadrics is:

$$\left(\frac{x}{a}\right)^n + \left(\frac{y}{b}\right)^n + \left(\frac{z}{c}\right)^n = 1 \quad (3)$$

The fractions b/a and c/a are the aspect ratios in the xy and xz directions respectively. For $a = b = c$ and $n = 2$, the resulting particle is a sphere. As n increases, the particle shape approaches that of a cube with progressively sharper corners.

The typical DEM algorithm tracks all particles and collisions within the system being modelled and collects the resulting forces on the particles and on the boundaries, so as to sufficiently resolve the contact dynamics. Several statistics relevant to energy dissipation are recorded for the purpose of investigating flow related mechanisms responsible for dissipation in the rolling container.

The particles used have size and shape parameters which are representative of sand particles as in the experiments. Their shapes are represented here by super-quadrics with blockiness parameter n randomly distributed with a uniform probability between 2.5 and 5.0. The super-quadric major axis length is distributed between 1.6 and 2.0 mm, and the super-quadric aspect ratios b/a and c/a between 0.8 and 1.0. The bulk material density is 1600 kg/m^3 . A spring stiffness k of 600 N/m was chosen to maintain average particle overlaps to be smaller than 0.5% of the particle radius. For both particle-particle and particle-boundary collisions, the coefficient of restitution was chosen as 0.75 and the coefficient of friction as 0.70 from simple experiments. The container object is a cylinder with inner radius of 37.5 mm and length of 200 mm. A 20% fill level corresponds to around 50,000 particles.

Dynamics of Sloshing Absorber

For the simulations presented here, we currently do not have a model for contact detection between different boundary objects and thus need to constrain the cylinder's path to follow the profile of the ramp. We do this by discretising the curved ramp into a piecewise linear representation. The ramp then becomes an assembly of linear segments that are input into the DEM solver as a sequence of horizontal positions and ramp angles. The ramp profile used is a 6th-order polynomial curve of best fit through measured coordinates on the real ramp. The cylinder object is constrained to follow the path of the ramp surface with a no-slip condition. At each time step the forces on the cylinder are calculated as the sum of the forces acting on the cylinder due to external and internal forces. The external forces are due to gravity for the current angle of the ramp, θ . The internal forces are due to particles acting on the internal cylinder boundary, represented by F_x , F_y and T_z . The total acceleration acting on the cylinder at each position in a direction parallel to the ramp at that position is given by:

$$ROTACC = \frac{1}{2} g \sin \theta + \frac{1}{2} F_x \frac{\cos \theta}{m} + \frac{1}{2} F_y \frac{\sin \theta}{m} + \frac{1}{2} \frac{T_z}{mr} \quad (4)$$

where m is the cylinder mass, r is the cylinder radius, F_x , F_y and T_z are the forces and the torque due to the particles acting on the cylinder. The forces and their directions are shown in Figure 3.

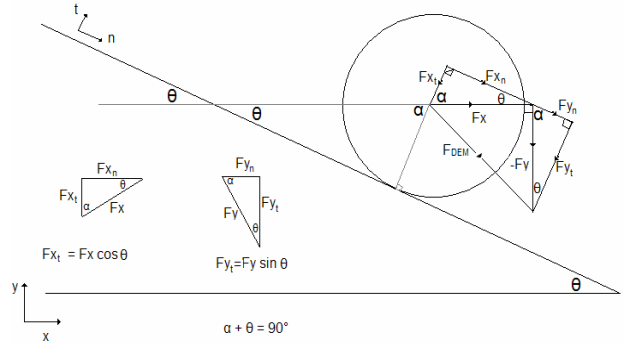


Figure 3. Diagram of the rolling cylinder, ramp and the relevant forces. Global coordinates are x, y . Local coordinates are n, t .

Numerical Predictions and Comparisons

Two simulations have been performed for this study. One where the motion of the container was fully specified to follow the motion of the container observed in prior experiments [8]. The other case makes use of the dynamic motion model described above to predict the container motion on the ramp. In Figure 4, the motion of the cylinder for the two simulation cases together with the experiment are shown. The comparison between the specified motion simulations and the experiment has shown a close match for the particle kinematics earlier as reported in Dragomir et al. [9].

The stopping distance for the container is completely defined in the specified motion case describing the position on the level plane of the ramp where the container in the experiments came to a complete stop. This distance is a measure of the total energy dissipated in the system. The stopping distance is dynamically predicted in the dynamic motion case, as a result of how much energy is dissipated in the container due to particle flow.

The container positions in both the horizontal and vertical directions are shown in Figure 5 for the dynamic and specified motion simulations. From this, we can see that the stopping distance in the dynamic motion prediction is over-estimated from the experiments by about 7%. Also, the total distance travelled along the vertical axis differs by 2 cm, which corresponds to a ramp error of approximately 8%. This may be attributable to one

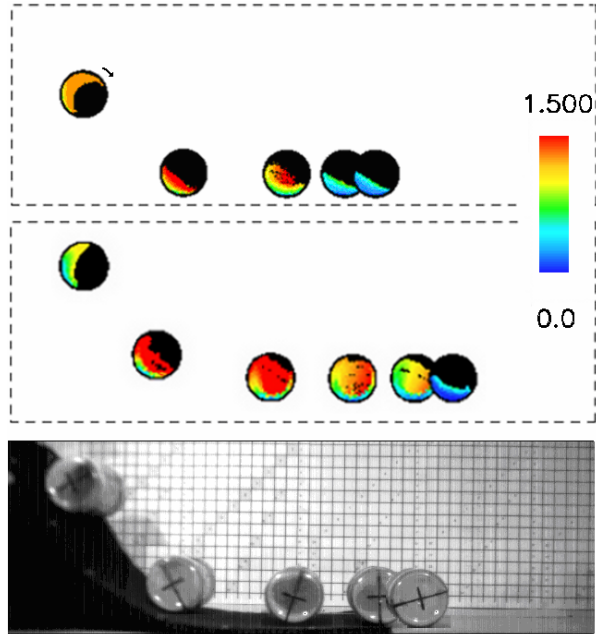


Figure 4. Motion of cylinder down ramp for specified case (top), dynamic model (middle) and for experiment (bottom).

of three potential sources of error: 1) measurement error in the process of measuring and digitising the ramp profile; 2) incorrect material specification for the particles (we have not yet investigated the sensitivity of the coupled particle-container motion to material properties and it is quite possible that these are not correct); and 3) potential slip between the container and ramp in the experiments. Despite the errors, the predictions from the dynamic motion case are in very good agreement with that determined from experiment and imposed in the specified case.

The container speed is tracked by the solver for the specified and dynamic motion cases as shown in Figure 6. Here, the step-wise discontinuous history corresponds to the specified motion measured at regular intervals throughout the experiment. The overall shape of the motion of the dynamic model and the specified motion model, is quite similar. There are, however, fluctuations in the dynamic model case which are discussed in the following section. Finally, the angular speed of the rolling container is shown in Figure 7. The trends closely follow those in Figure 6 since the linear and angular motions are fully coupled due to the no-slip condition in the dynamic motion case.

Energy Dissipation Events

It has been noted earlier that three distinct events, associated with cataracting particle flow, can be identified for the case given in Figure 4 [9]. These are marked as (1), (2) and (3) in Figure 8 which shows the input power to the container due to torque exerted on the container by the particles. The black line corresponds to the specified motion case, while the red line corresponds to the dynamic motion case in this figure. There is substantial difference in the power between the 2 cases. The

dynamic case appears to experience greater torque on the boundary which indicates that the behaviour of the particle flow and the forces exerted onto the container are different for the specified and dynamic motion cases. The dynamic case predicts four dissipative (high power) events, marked as (a), (b), (c) and (d), and these occur at roughly the same times as in the specified simulation.

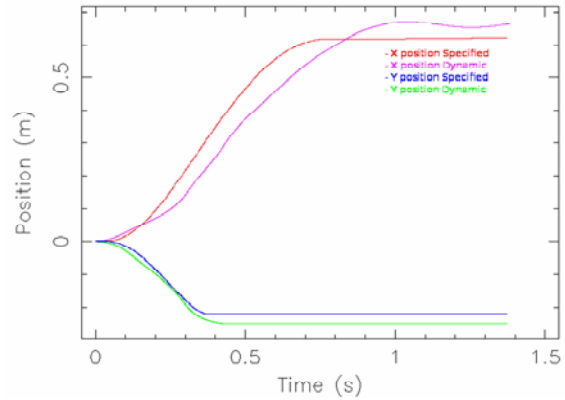


Figure 5. Histories of the container x and y position for the specified and dynamic motion cases.

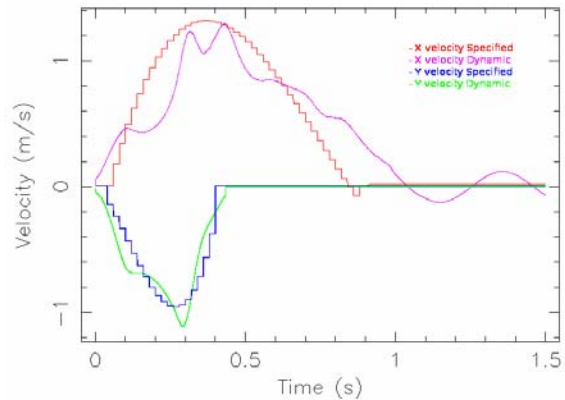


Figure 6. Histories of the container x and y velocity for the specified and dynamic motion cases.

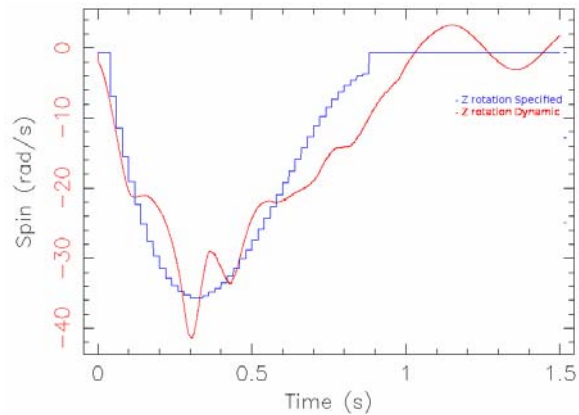


Figure 7. History of the container angular speed for the specified and dynamic motion cases.

Event (3) for the specified case has a much higher magnitude than the corresponding event (d) for the dynamic case. This is due to abruptly stopping the container in the specified case.

The dynamic case requires a longer stopping time as the particles have to dissipate the residual energy through collisions, after the level portion is reached. This difference in the residual energy can be attributed to the surface on which the experiment was performed which could not be guaranteed to be non-slip, dissipating some energy at the contact point between the container and the ramp surface.

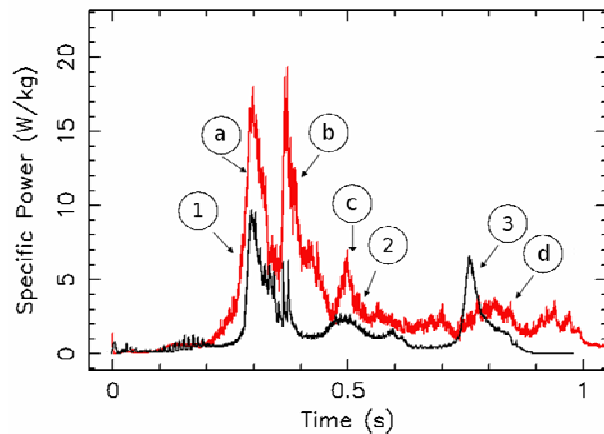


Figure 8. History of the input power to the system due to the particle torque on the container boundary for the dynamic case (red) and the specified case (black).

The fluctuating motion experienced by the container in the dynamic model seen in Figure 6 and 7 is clearly the effect of the 2-way communication between the particles and the cylinder. For the case of the vertical motion, there is an increase in speed as the container descends the ramp. The effect of the particle motion on the container is easily observed for the dynamic case. Events (a) and (b) in Figure 8 describe sloshing events with the container accelerating, decelerating and then accelerating again (see Figure 6) in response to the internal flow. For the specified case, there is only a single event (1) as the cylinder does not move in response to this flow and therefore damps out the sloshing motion. These events dissipate energy and there is a clear relationship between the power peaks and the structure of the velocity profiles in Figure 6 and 7.

During the development of the dynamic model, one very important factor on stopping distance, particle kinematics and overall energy in the system has become obvious. It is very important that the ramp geometry is accurately represented as the boundary condition for the rolling container. Some of the unexplained differences in the particle kinematics will be due to the inability to best measure and represent the real ramp by a polynomial curve. This point is currently under development to avoid such difficulties.

Conclusions

This paper shows that, while a specified-motion simulation can accurately predict the particle kinematics, a dynamic model can offer additional insight into the workings of the flow for a cylindrical rotating container partially filled with a granular

material. The dynamic case describes aspects of the container motion not easily observable from the experiment. These have been shown to be related to structure in the input power (and internal dissipation) in this system. The dynamic model thus offers a better tool for understanding the dissipation mechanisms of this complex system.

Presented work should be interpreted as a qualitative assessment of the numerical prediction tool. A relatively close prediction of the true stopping distance is an encouraging result and indicates the potential of the model as a powerful design tool for practical implementation.

References

- [1] Barker, C. G., Computer simulations of granular materials, *Granular Matter, A Interdisciplinary approach*, Ed. A. Mehta, Springer, NY, 1994, 35-84.
- [2] Campbell, C. S., Granular material flows - An overview, *Powder Technology*, **162**, 2006, 208-229.
- [3] Cleary, P. W., Predicting charge motion, power draw, segregation, wear and particle breakage in ball mills using discrete element methods, *Minerals Engineering*, **11**, 1998, 1061-1080.
- [4] Cleary, P. W., Recent advances in DEM modelling in tumbling mills, *Minerals Engineering*, **14**, 2001, 1295-1319.
- [5] Cleary, P. W., The effect of particle shape on simple shear flows, *Powder Technology*, **179**, 2008, 144-163.
- [6] Cleary, P. W., and Sinnott, M. D., Assessing mixing characteristics of particle-mixing and granulation devices, *Particology*, **6**, 2008, 419-44.
- [7] Dragomir, S. C., Semercigil, E. S., Turan, O. F., (2007) "Induced Particle Sloshing In A Rotating Container, 16th Australasian Fluid Mechanics Conference, 1207-1212.
- [8] Dragomir, S. C., Sinnott M., Semercigil, E. S., Turan, O. F., (submitted 2010), "Energy Dissipation Characteristics of Particle Sloshing in a Rotating Cylinder", *Journal of Sound and Vibration*.
- [9] Dragomir, S. C., Sinnott M., Semercigil, E. S., Turan, O. F., Predicting Energy Dissipation Characteristics of a Tumbling Granular-Flow Damper Using DEM, 7th International Conference on CFD in the Minerals and Process Industries, December 2009.
- [10] Sinnott, M., Cleary, P. W., and Morrison, R., Analysis of stirred mill performance using DEM simulation: Part 1 - Media motion, energy consumption and collisional environment, *Minerals Engineering*, **19**, 2006, 1537-1550
- [11] Walton, O. R., Numerical simulation of inelastic frictional particle-particle interaction, *Particulate two-phase flow*, Ed. M. C. Roco, Butterworth-Heinemann, 1992, 884-911.